Carbohydrate Polymers 111 (2014) 928–935

Contents lists available at ScienceDirect

Carbohydrate Polymers

journal homepage: www.elsevier.com/locate/carbpol

A novel melphalan polymeric prodrug: Preparation and property study

Dan Li[a], Bo Lu[a,b,*], Zhijun Huang[a,b], Peihu Xu[a,b], Hua Zheng[a,b], Yihua Yin[a], Haixing Xu[a,b], Xia Liu[a], Lingyun Chen[c], Yiceng Lou[a], Xueqiong Zhang[a], Fuliang Xiong[a,b]

[a] Department of Pharmaceutical Engineering, School of Chemical Engineering, Wuhan University of Technology, Wuhan 430070, PR China
[b] Engineering Technology Center of Hubei traditional Chinese Medicine Preparation, Wuhan University of Technology, Wuhan 430070, PR China
[c] Department of Agricultural, Food and Nutritional Science, University of Alberta, Edmonton, Canada T6G 2P5

ARTICLE INFO

Article history:
Received 26 October 2013
Received in revised form 15 April 2014
Accepted 19 April 2014
Available online 20 May 2014

Keywords:
Carboxymethyl chitosan
Cathepsin X
Melphalan
Nanoparticles

ABSTRACT

The clinical application of melphalan (Me), an anticancer drug for the treatment of hematologic malignancies, has been limited due to its poor water solubility, rapid elimination and lack of target specificity. To solve these problems, *O*,*N*-carboxymethyl chitosan–peptide–melphalan conjugates were synthesized and characterized. All polymeric prodrugs showed satisfactory water solubility. It was found that the molecular weight of *O*,*N*-carboxymethyl chitosan (*O*,*N*-CMCS) and the peptide spacer played a crucial role in controlling the drug content, diameter and drug release properties of *O*,*N*-carboxymethyl chitosan–peptide–melphalan conjugates. The studies of in vitro drug release and cell cytotoxicity by MTT assay revealed that, employing the polymeric conjugation strategy and using the peptides glycylglycine (Gly-Gly) as a spacer, the conjugates have good cathepsin X-sensitivity and lower toxicity and the drug release behavior improved remarkably. In conclusion, *O*,*N*-carboxymethyl chitosan–peptide–melphalan conjugates could be promising prodrugs for anticancer application.

1. Introduction

Recent advances in prodrug have led to the development of controlled drug delivery systems with desirable properties that can overcome the limitations of traditional therapeutic agents (Bildstein, Dubernet, & Couvreur, 2011; She et al., 2013; Chhikara, Mandal, & Parang, 2010). Various water-soluble polymers and their conjugates with peptides are used as carriers for improving the utilization of anticancer agents. A successful drug delivery system relies on an appropriate selection of the polymer carrier, targeting residues and the linkage spacer (Jain, Kesharwani, Gupta, & Jain, 2012). The release rate of prodrugs can be controlled by site-specific hydrolysis.

Prodrugs combining therapeutic agents and targeting residues are an emerging technique to improve the therapeutic effect of hematologic malignancies. Among hematologic malignancies, there are over two-dozen drug delivery systems that have been developed for treating leukemia. However, only a limited number of systems have been developed targeting multiple myeloma (Dinauer et al., 2005; Parekh, Weniger, & Wiestner, 2011; Zheng et al., 2011). Multiple myeloma (MM) is a relatively common clonal B-cell malignancy (Mincher et al., 2008). MM accounts for 13.4% of all hematologic malignancies diagnosed, 19% of all deaths resulting from hematologic malignancies, and 2% of all cancer deaths (Mahindra, Hideshima, & Anderson, 2010).

Melphalan (Me) is an anticancer drug for the treatment of hematologic malignancies, especially multiple myeloma and chronic lymphocytic leukemia (Hjertner, Börset, & Waage, 1996; Machana, Weerapreeyakul, Barusrux, Thumanu, & Tanthanuch, 2012). Melphalan exhibits beneficial treatment effect, and the major disadvantages are poor water solubility and lack of target specificity. Most studies are concentrated on chemical modifications and formation of prodrugs or nanosystems to reduce the toxicity of melphalan (Wickström et al., 2010; Rajpoot, Bali, & Pathak, 2012). Although the water solubility and toxicity of melphalan have been improved in these studies, only limited efforts have been focused on its targeted delivery.

Higher expression of unique enzymes in cancer cells than in normal cells can be exploited for development of site-selective delivery systems (Vig, Huttunen, Laine, & Rautio, in press). Many

* Corresponding authors at: Department of Pharmaceutical Engineering, 122 Luoshi Road, Wuhan, Hubei, Wuhan 430070, PR China. Tel.: +86 27 87859019; fax: +86 27 87859019.
E-mail addresses: whulb@163.com (B. Lu), whutlvb@163.com (H. Zheng).

http://dx.doi.org/10.1016/j.carbpol.2014.04.062
0144-8617/

cathepsin-sensitive peptides were invoked as spacers and linked with anticancer drugs such as paclitaxel, doxorubicin, methotrexate, geldanamycin, solamargine (Burke et al., 2009; Liang et al., 2012; Sun et al., 2010; Jeffrey et al., 2006; Ofner, Pica, Bowman, & Chen, 2006). Ruth et al. (1991) have proved that *P*-Gly-Phe-Leu-Gly-Me had a response toward cathepsin B (CB) in terms of melphalan release. Moreover, proline prodrugs of melphalan (Chrzanowski, Bielawska, & Pałka, 2003) and methotrexate (Wu, Shah, Patel, & Yuan, 2010) were designed for their targeted delivery to tumor cells where the spacers can be cleaved by specific enzymes (imidodipeptidase and prolidase, respectively) to release the conjugated drugs.

Cathepsin X belongs to the papain family of cysteine proteases and is over-expressed in cancer cells (Nägler and Ménard, 1998; Obermajer, Doljak, Jamnik, Fonović, & Kos, 2009; Kirschke, 2007). More recent findings indicate that cathepsin X can release C-terminal amino acids of polypeptides and proteins and has the possibility of being used for development of cancer therapy (Paulick & Bogyo, 2011; Nägler et al., 1999). For example, glycylglycine peptides (Gly-Gly) were intended to be a highly specific substrate for cathepsin X and the linkage between the polymer and the drug (Devanathan et al., 2005).

In this work, *O*,*N*-CMCS-(Gly-Gly)$_n$-Me prodrug with Gly-Gly as a cathepsin X substrate was synthesized. Then nanoparticles were formed by self-assembly of *O*,*N*-CMCS-(Gly-Gly)$_n$-Me polymers. Morphology and size of nanoparticles, in vitro drug release, and cell cytotoxicity of the polymeric prodrugs were investigated to demonstrate the importance of molecular weight of polymers and the effect of spacer in design of polymeric prodrugs.

2. Materials and methods

2.1. Materials

Carboxymethyl chitosan (CMCS) was acquired from Jinke Zhejiang, China. Melphalan was provided by Suzhou Lide Inc. China. *N*,*N*-dimethylformamide (DMF), 1,4-diethylene dioxide, 1-ethyl-(3-dimethyllaminopropyl) carbodiie hydrochlide (EDC·HCl), *N*-hydroxysuccinimide (NHS), dimethyl sulfoxide (DMSO), ethylene diamine tetraacetic acid (EDTA) and glutathione (GSH) were recruited from National Medicines (Group) Co., Ltd, and purified before use. Fmoc *N*-hydroxysuccinimide este (Fmoc-OSu), *N*,*N*′-diisopropylcarbodiimide (DIC), *O*-benzotriazole-*N*,*N*,*N*,*N*-tetramethyl-uronium-hexafluorophosphate (HBTU), 4-dimethylaminopyridine (DMAP) and *N*,*N*-diisopropylethylamine (DIEA) were purchased from Shanghai Medpep (Group) Co., Ltd. All the other chemicals were of analytical or reagent grade and were obtained from commercial channels without any purification. Ultrapure deionized water was used in all buffer solutions and experiments.

2.2. Cell lines and culture conditions

The RPMI8226 human myeloma cell line was obtained from American Type Culture Collection (ATCC, Rockville, MD, USA) and maintained in RPMI1640 medium containing 10% fetal bovine serum (FBS) (Gibco, Grand Island, NY, USA), 100 units/ml penicillin, and 100 g/ml streptomycin at 37 °C with 5% CO_2. The cells for experiments were in their logarithmic growth phase.

2.3. Synthesis of O,N-CMCS-(Gly-Gly)$_3$-Me delivery system

2.3.1. Synthesis of Fmoc-(Gly-Gly)$_n$ and Fmoc-Melphalan

Fmoc-(Gly-Gly)$_n$ was synthesized by mixing Gly-Gly 1.0 mmol and Fmoc-OSu 1.2 mmol in 1,4-diethylene dioxide 20 ml at room temperature under constant stirring for 24 h. The reaction mixtures were diluted with 150 ml deionized water and extracted with ether. The extraction was dissolved again, 12% (v/v) HCl was used for acidization with the aqueous phase. The precipitate was collected, cooled over night and then washed with acetic ester, deionized water and saturated sodium chloride solution, and finally dried under vacuum. Fmoc-Melphalan was synthesized by the same method as Fmoc-(Gly-Gly)$_n$.

2.3.2. Synthesis of (Gly-Gly)$_n$-Me

Fmoc-Melphalan (1 mmol) was in addition to Wang resin (4-(Hydroxymethyl) phenoxymethyl Polystyrene Resin, 2.0 g) after 5 min of preactivation in DMF using DMAP (150 mg) and DIC (100 mg) as catalysts. After washing with DMF (4–6 times with 20 ml), piperidine solution was inserted twice for 5 + 10 min to remove Fmoc- group and then washed in DMF. Fmoc-(Gly-Gly)$_n$ (0.5 mmol), HBTU (3 mmol) and DIEA (0.5 ml) were added to react for 40 min and followed by washing with DMF. The product was cleaved from the resin with pyridine, neutralized with acetic anhydride (volume ratio of 1:1) and purified by preparative RP-HPLC. Removed from Wang resin, Fmoc-(Gly-Gly)$_n$-Me was dissolved in 20 ml dichloromethane with 10 times amount of diethylamine as a catalyst at room temperature under constant stirring for 24 h. Subsequently, the solids were purified by crystallization in a solvent of petroleum ether, thoroughly washed with deionized water, and dried under vacuum to afford the desired product as a white powder (yield = 34%).

2.3.3. Synthesis of O-CMCS-(Gly-Gly)$_3$-Me

O-CMCS (600 mg) was suspended in 15 ml of ultrapure deionized water using EDC·HCl (260 mg, 1 mmol) and NHS (230 mg, 1.05 mmol) as couple reagents for activation of carboxyl group. After 6 h, (Gly-Gly)$_3$-Me (300 mg, 0.5 mmol) were dissolved in 5 ml DMSO and was added to the reaction system dropwise. The reaction mixture was stirred at room temperature for 24 h. After dialysis and lyophilization, the products were obtained as a white fibrous (62% yield).

2.3.4. Synthesis of O,N-CMCS-(Gly-Gly)$_3$-Me

O-CMCS-(Gly-Gly)$_3$-Me (2.5 g) dissolved in 30 ml isopropanol. After 1 h, an aqueous NaOH solution (10 ml, 40% w/v) was added dropwise into the reaction system at 30 °C. The emulsion was stirred overnight for alkalization. Chloroacetic acid (12 g, 0.13 mol) in a 20 ml isopropanol was slowly added to this solution at 60 °C. The reaction mixture was stirred for 3 h until a uniform solution was obtained. 15 ml 1 M NaOH was used to neutralize and the crude product was precipitated by ethanol. The attained solid was dissolved in 500 ml ultrapure waters. Hydrochloric acid was used to adjust pH to the isoelectric point. White precipitation appeared was washed twice with ethanol. The white fibrous products in 77% yield were achieved after vacuum drying at 50 °C.

2.4. Characterization of (Gly-Gly)$_3$-Me and CMCS-(Gly-Gly)$_3$-Me

2.4.1. Mass spectrometric analysis of (Gly-Gly)$_3$-Me

LC–MS/MS was performed using 1100 LC/MSD Trap mass spectrometer (Agilent, USA) equipped with an Accela pump and a deconvolution software. Electrospray-ionization was performed in the negative ion mode. Nitrogen was used as nebulizer gas set at 1.5 l/min. The mobile phase was 50% H_2O and 50% ACN with a flow rate of 0.2 ml/min. The spray voltage was 3.5 kV, DL temperature 250 °C, block temperature 200 °C.

2.4.2. FTIR of CMCS-(Gly-Gly)$_3$-Me

The IR spectra of (Gly-Gly)$_3$-Me and CMCS-(Gly-Gly)$_3$-Me conjugates were measured on a FT-IR spectrometer (Bruker TENSOR 27, German) using KBr pellets.

2.4.3. NMR of CMCS-(Gly-Gly)$_3$-Me

(Gly-Gly)$_3$-Me and CMCS-(Gly-Gly)$_3$-Me were lyophilized and re-dissolved in deuterated DMSO (d_6-DMSO) and D_2O and characterized by ^{1}H NMR at 500 MHz and ^{13}C NMR at 100 MHz (Mercury Plus 400, Varian, USA).

2.4.4. Determination of drug loading capacity

Content of incorporated melphalan was determined by measuring the UV absorption of the conjugate solution in distilled water at 263 nm. The reference solution having the identical solvent with the test solution was prepared. Me content was identified with the help of a calibration curve of Me in a mixture solution (methanol:water:acetic acid = 49.5:49.5:1) range from 2 to 50 μg/ml with r^2 = 0.99636. Me content was calculated as follows:

$$\text{Me\%} = \left(\frac{m_{\text{Me}}}{m_{\text{prodrug}}}\right) \times 100\%$$

2.5. Preparation of O,N-CMCS-(Gly-Gly)$_3$-Me nanoparticles

O,*N*-CMCS-(Gly-Gly)$_3$-Me polymer dissolved in pH 7.4 phosphate-buffered saline (PBS) to the desired concentration (10 mg/ml) with uninterrupted magnetic stirring. Then it was sonicated twice at 100 W for 4 min, using a probe-type sonifier (JY92-2D, Ningbo Scientz Biotechnology CO., Ltd, China). To protect the solution from heat build-up, a pulse function was used (pulse on, 2.0 s; pulse off, 2.0 s).

2.6. Characterization of nanoparticles

2.6.1. Measurements of critical micelle concentration

The critical micelle concentration (CMC) of the copolymers was established by fluorescence spectroscopy using pyrene as a fluorescence probe (Cammas et al., 1997; Jie, Venkatraman, Min, Freddy, & Huat, 2005). Pyrene solution in methanol (0.22 g/l) was put into vials. Methanol was evaporated by a nitrogen stream. Nanoparticles solutions in water were added to the vials containing pyrene ([py] = 6.0×10^{-7} M). The concentration of micelles ranged from 10 mg/ml to 0.01 mg/ml. The mixture was stored overnight for equilibrium. Emission spectra (λ_{em} = 350–450 nm, λ_{ex} = 335 nm, E_x(SBW) = 3 nm, E_m(SBW) = 1.5 nm) were accounted for. Upon formation of nanoparticles, pyrene would move into the inside of the nanoparticles from the aqueous phase which is expected to result in an alteration in the intensity ratio (I_1/I_3) of pyrene fluorescence bands I (372 nm) and III (383 nm).

2.6.2. Particle size, morphology, and zeta-potential of nanoparticles

The morphology of the self-aggregate sample was obtained by transmission electron microscopy (TEM) analysis using JSM-6700F, made by JEOL, Japan operated at 200 kV. To prepare the TEM sample, a drop of solution (5 mg/ml) was deposited onto 200 mesh copper grids and dried at room temperature.

The average particle size and size distribution were determined by dynamic light scattering (DLS) analysis using a Malvern Zetasizer Nano ZS (Malvern, UK) at a polymer concentration of 5 mg/ml. The nanoparticles were sonicated before measurement. DLS measurements were performed at least in triplicate for each sample.

2.7. In vitro drug release

O,*N*-CMCS-(Gly-Gly)$_3$-Me dissolved in 0.15 M PBS (pH = 5.5) was put in the release media (1 ml) containing rat liver tritosomes to initiate the release of melphalan. The medium without enzyme or tritosomes was used as a control sample. The tritosomes were extracted from the liver of Kunming strain mice (20 ± 2 g) supplied by Hubei Experimental Animal Center (Juan & Bonifacino, 2009). The release studies were carried out for 24 h at an oscillation condition of 37 °C, 50 rpm. At specific time intervals, 10 μl samples were withdrawn and analyzed with HPLC and concentrations of melphalan were determined using the standard curve prepared under the same conditions. Various tritosomes concentrations were used to determine tritosomes dependent release kinetics of *O*,*N*-CMCS-(Gly-Gly)$_3$-Me.

Prodrug was also incubated at a concentration of 100 μM with 5×10^{-6} M papain suspension in 0.1 M PBS (pH = 5.5). EDTA (1 mM) and GSH (1 mM) were added to activate papain. The mixture was incubated at 37 °C. The papain dependent release was also determined by the same method as the tritosomes dependent release.

High performance liquid chromatography (Agilent 1100N, USA) was used for analysis of melphalan release in medium with different enzymes (Pinguet et al., 1996). The eluent mixture was comprised of methanol, purified water and acetic acid (49.5:49.5:1, v/v) and deaerated by ultrasound prior to use. The mobile phase was pumped onto the column at 1.0 ml/min, which corresponds to a pressure of about 120 bar. The volume injected was 20 μl, the chromatography was performed at 35 °C and the analytes were detected at 254 nm. The calibration curve was found to be linear in the range of 0.1–50 μg/ml with the r^2 value of 0.9966.

2.8. Cell cytotoxicity assays

Evaluation of the cytotoxicity of polymers was performed by MTT method (Mao, Ma, Zhou, Gao, & Shen, 2005). The RPMI8226 human myeloma cells were seeded in the 96-well plate at a density of 4×10^5 cells/well in 100 μl DMEM containing 10% fetal bovine serum (FBS), 100 units × ml^{-1} penicillin, and 100 g × ml^{-1} streptomycin. After incubation for 24 h, polymer solutions were added to the culture medium. Cell viability was tested after the addition of polymer for 48 h. After incubation, 10 μl MTT (5 mg/ml) solution in PBS (pH = 7.4) was added to each well and further incubated in 5% CO_2 incubator at 37 °C for 4 h. After removal of the MTT containing medium, 100 μl DMSO was added to dissolve the formazan crystals formed in living cells. Finally, the absorbance was measured at 490 nm using a microplate reader (BIO-RAD, Model 550, USA). The relative cell viability was calculated as: Cell viability (%) = (OD_{sample})/($OD_{control}$) × 100, where $OD_{control}$ (control optical density) was obtained in the absence of polymers and OD_{sample} (optical density of the sample) was obtained in the presence of polymers. Cells incubated in the absence of nanoparticles were used as a control. Each value was averaged from 6 parallel experiments.

2.9. In vitro cellular uptake

The cellular uptake of *O*,*N*-CMCS-(Gly-Gly)$_3$-Me nanoparticles by cancer cells were supported by a confocal laser scanning microscope (FV1000 confocal laser scanning microscope (CLSM), Olympus Corporation, Tokyo, Japan) (Anitha et al., 2011). The RPMI8226 human myeloma cells were seeded in a 24-well tissue culture plate at a density of 10^6 cells per well, and were allowed to grow for 24 h. In order to characterize cellular uptake of *O*,*N*-CMCS-(Gly-Gly)$_3$-Me nanoparticles, the nanoparticles were fluorescently labeled with Dylight-488 dye. After 24 h of growth, the nanoparticles were added into the culture plate and incubated at 37 °C for 1 h. After incubation, the cells were washed with PBS. The cells were centrifuged, and the supernatant was discarded. The cells were resuspended in PBS solution, and subsequently measured.

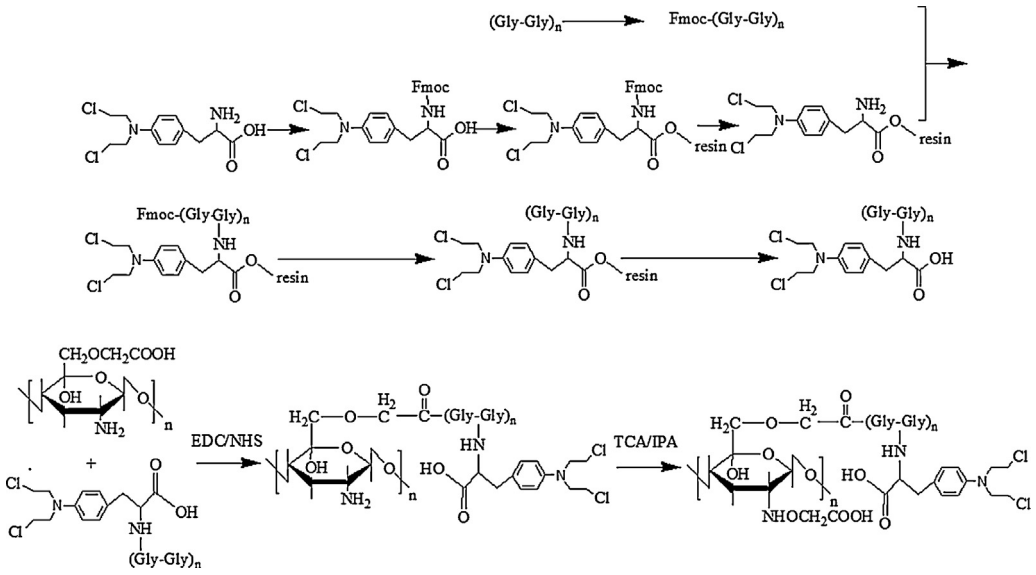

Scheme 1. Synthesis route of *O*,*N*-CMCS-Gly-Gly-Me.

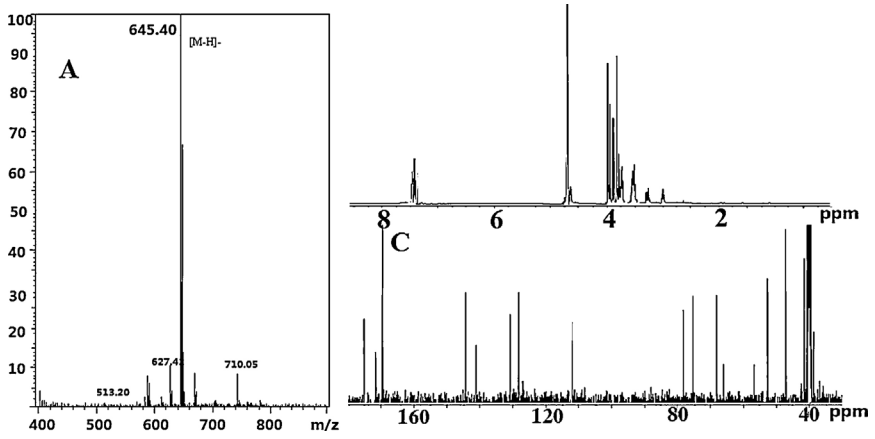

Fig. 1. Spectra of $(Gly\text{-}Gly)_3$-Me and *O*,*N*-CMCS-$(Gly\text{-}Gly)_3$-Me. (A) MS spectra of $(Gly\text{-}Gly)_3$-Me; (B) ^1H NMR spectra of *O*,*N*-CMCS-$(Gly\text{-}Gly)_3$-Me in D_2O; (C) ^{13}C NMR spectra of *O*,*N*-CMCS-$(Gly\text{-}Gly)_3$-Me in d_6-DMSO.

3. Discussion and results

3.1. Synthesis and characterization of $(Gly\text{-}Gly)_n$-Me and *O*,*N*-CMCS-$(Gly\text{-}Gly)_n$-Me

Sample preparation procedures were illustrated in Scheme 1. $(Gly\text{-}Gly)_n$-Me was prepared by solid phase peptide syntheses. To synthesize *O*,*N*-CMCS-$(Gly\text{-}Gly)_n$-Me prodrug, the C6-carboxyl group of *O*-CMCS was firstly activated by NHS and then chemically coupled with the amino group of $(Gly\text{-}Gly)_n$-Me by formation of an amide bond using "zero length" crosslinker of NHS. Then making $n = 3$ as an example for structure analysis.

As showed in Fig. 1A, the measured molecular weight as revealed by MS data is consistent with the value of $(Gly\text{-}Gly)_3$-Me. The samples were further analyzed by FTIR and NMR spectroscopy. In comparison to the melphalan spectrum (Fig. 2A), additional absorption bands were observed for $(Gly\text{-}Gly)_3$-Me (Fig. 2C) at 1617 cm^{-1}(amide II band C=O stretch), 1546 cm^{-1}(amide II band N—H bend). Meanwhile, the characteristic absorptions of melphalan remained at: 3418 cm^{-1}(—NH_2 stretch), 2961 cm^{-1} (—OH, —CH_2, C—H stretch), 1518 and 1443 cm^{-1} (C=C stretch), 1348 cm^{-1} (C—N stretch), 806 cm^{-1} (C—H bend of benzene ring), and 745 cm^{-1} (C—Cl stretch).

Fig. 2B and D shows the FT-IR spectra of CMCS and *O*,*N*-CMCS-$(Gly\text{-}Gly)_3$-Me prodrug, The band assignment of CMCS is as follows: 3450–3408 cm^{-1} (O—H stretch overlapped with N—H stretch), 2851 cm^{-1} (C—H stretch), 1630 cm^{-1} and 1431 cm^{-1} (COO^- antisymmetric and symmetric stretch), 1315 cm^{-1} (C—N stretch), 1240 cm^{-1} (bridge O stretch), 1082 cm^{-1} (C—O—C stretching vibration in the glucopyranose ring). Compared to CMCS (Fig. 1B), the bands of *O*,*N*-CMCS-$(Gly\text{-}Gly)_3$-Me (Fig. 1D) at 3330–3320 cm^{-1} (O—H stretch overlapped with N-H stretch) and 1650–1550 cm^{-1} (C—O stretch overlapped with N—H bend) obviously increase. New absorption band of *O*,*N*-CMCS-$(Gly\text{-}Gly)_3$-Me at 1240 cm^{-1} (C—H stretch of the benzene ring), 1576 cm^{-1} (amide II band N—H bend) appears.

In the ^1H NMR spectrum of *O*,*N*-CMCS-$(Gly\text{-}Gly)_3$-Me (Fig. 1B), the peaks at 7.37 ppm and 7.44 ppm in ^1H-NMR correspond to the protons in the benzene ring and the amide bond protons linking glycylgcine with melphalan. The signal at 3.5–4.0 ppm corresponds to the saccharide ring and carboxymethyl group protons of *O*,*N*-CMCS, —$N(CH_2CH_2)_2$ groups and —CH_2 of glycine. In Fig. 1C, the peaks at 60–80 ppm in ^{13}C-NMR correspond to the carbons in the saccharide ring of *O*,*N*-CMCS. The signal at 169.6 ppm corresponds to the carbons of glycine. The peak at 111.9 ppm is from the —$N(CH_2CH_2)_2$ groups of melphalan. These results indicate that the

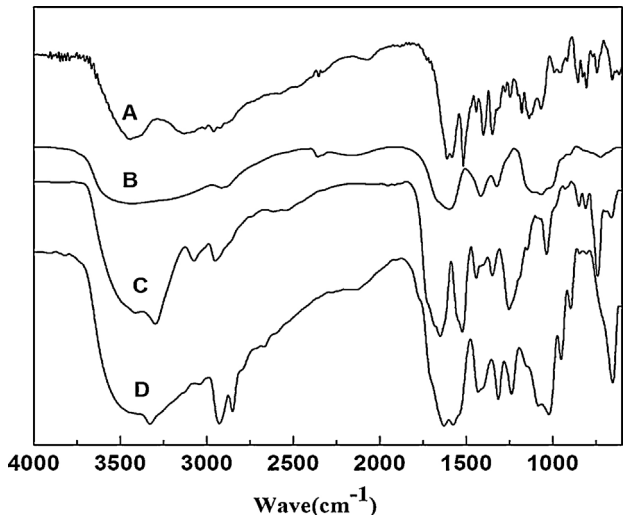

Fig. 2. FTIR spectra: (A) Melphalan; (B) CMCS; (C) $(Gly\text{-}Gly)_3$-Me; (D) *O,N*-CMCS-$(Gly\text{-}Gly)_3$-Me).

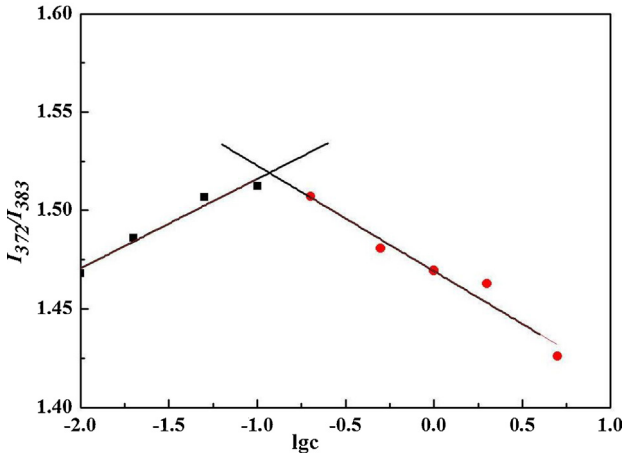

Fig. 3. The relationship of I_{372}/I_{383} from fluorescence spectra of pyrene (6×10^{-7} M) with lgC of *O,N*-CMCS-$(Gly\text{-}Gly)_3$-Me.

polymer prodrug *O,N*-CMCS-$(Gly\text{-}Gly)_3$-Me was synthesized successfully.

The weight percentage (wt%) of Me in the *O,N*-CMCS-$(Gly\text{-}Gly)_3$-Me conjugates was analyzed using a UV spectrophotometer by measuring absorption at a wavelength of 263 nm. As showed in Table 1, the drug loading content reduces from 12.22 to 6.17% with increasing the molecular weight from 6.0×10^4 to 3.4×10^8. This may be attributed by the level of chain extension during the synthesis process. The results indicate that the Me content of *O,N*-CMCS-$(Gly\text{-}Gly)_3$-Me conjugates could be related to their molecular weight.

3.2. Characterization of O,N-CMCS-$(Gly\text{-}Gly)_3$-Me nanoparticles

It is noted that amphiphilic polymers with an appropriate hydrophilic/hydrophobic balance can self-assemble into nanoparticles in aqueous media. The amphiphilic *O,N*-CMCS-$(Gly\text{-}Gly)_3$-Me polymers, consisting of carboxyl and Me segments, were easily self-assemble into nanoparticles in PBS solutions. During preparation, there was no drug released from the polymers in aqueous media determined by HPLC. This demonstrates that the resulting nanoparticles are stable. Since pyrene is hydrophobic and has a very low solubility in water, it tends to solubilize in the hydrophobic region of nanoparticles, and the fluorescence intensity will be influenced by environmental change around pyrene. It is reported that the intensity ratio (I_{372}/I_{383}) of first (372 nm) and third (383 nm) peaks in the emission spectra is quite sensitive to the environmental change of pyrene. Therefore, this parameter was analyzed for determining critical micelle concentration (CMC) of *O,N*-CMCS-$(Gly\text{-}Gly)_3$-Me. As showed in Fig. 3, the intersection point of the two straight lines represents the critical micelle concentration, and CMC value was 0.1170 mg/ml.

A small enough particle size is an important prerequisite to enhance the cellular uptake of nanoparticles. Particle size of the nanoparticles was estimated by TEM. Fig. 4 displayed the morphology and size of the nanoparticles of *O,N*-CMCS-$(Gly\text{-}Gly)_3$-Me in PBS solutions. The typical images show that the nanoparticles in PBS solutions took near spherical shape and had no obvious agglomeration. Moreover, the nanoparticles possess a particle size of roughly 20–120 nm obtained by TEM images. However, the size was smaller than that measured by DLS, shown in Table 1. This might be mainly due to the process involved in the preparation of the sample. TEM images depict the actual size at the dried state of the sample, whereas the size measured by laser light scattering method is a hydrodynamic diameter (hydrated state). The nanoparticles showed a larger hydrodynamic volume due to the hydration effects (She et al., 2013). Compared with freshly prepared, the nanoparticles have no obvious change when stored at 4 °C in a PBS solution for one month (still 20–120 nm in diameter), which indicates that the nanoparticles had excellent stability (shown in Fig. 4).

In addition, characterization of nanoparticles with different polymer molecular weight was measured, shown in Table 1. The mean size of nanoparticles increased from 80 to 160 nm with the increase of molecular weight from 6.0×10^4 to 3.4×10^8. These results suggest that the mean size could be controlled by choosing polymer molecular weight to match requirements. The nanoparticles had a negative zeta potential (from −19.6 mV to −11.8 mV). It may be attributed to carboxyl groups on the particle surface.

3.3. In vitro drug release

Prodrugs were incubated with a model enzyme papain, cathepsin X and rat liver lysosomal enzymes (tritosomes) to study the drug release profiles. The in vitro drug release profiles from nanoparticles were shown in Fig. 5. Melphalan was continuously released up to 20 h, and the drug release rate varies depending on the enzyme used. Melphalan is being released more rapidly from nanoparticles incubated with cathepsin X and tritosomes (50%) than with papain (25%), suggesting that a cathepsin X-sensitive system has been successfully prepared (Fig. 5A, D and F). In addition, Fig. 5E–G displays an increasing drug release rate with longer spacer. This may be attributed that the longer spacer arm prevented steric hindrance and accelerated the drug release. The self-assembly process and drug release are displayed in Fig. 6. Amphiphilic copolymers can self-assemble into core-shell nanoparticles in aqueous environment. Thus the melphalan release from the polymeric prodrugs mainly depends on the type of enzyme. Therefore, this cathepsin X-sensitive system could be applied to enhance drug delivery.

In larger nanoparticles with the molecular weight of 2.5×10^7 and 3.4×10^8, 39% and 46% of melphalan had released from the particles after 10 h, respectively (Fig. 5B and C). In the small size groups with the molecular weight of 6.0×10^4, only 24% of drug was released (Fig. 5A). At the end of 20 h, no significant difference was observed in drug release levels. The drug release appears to be controlled by the swelling behavior of the nanoparticles. The larger nanoparticles swelled faster, resulting in the difference in drug release before 10 h. The release is only due to enzymatic

Table 1
Loading capacity and particle size of nanoparticles ($n = 3$).

Molecular weight	Drag content (%)	Restored time (d)	Diameter (mn)	PDI	Zeta potential (mV)
6.0×10^4	12.13	1	81 ± 6	0.402	−19.6
6.5×10^5	12.07	1	83 ± 4	0.247	−11.8
2.5×10^7	8.99	1	122 ± 3	0.556	−13.0
3.4×10^8	6.08	1	158 ± 4	0.265	−13.6
6.5×10^5	–	15	127 ± 6	0.538	−13.7

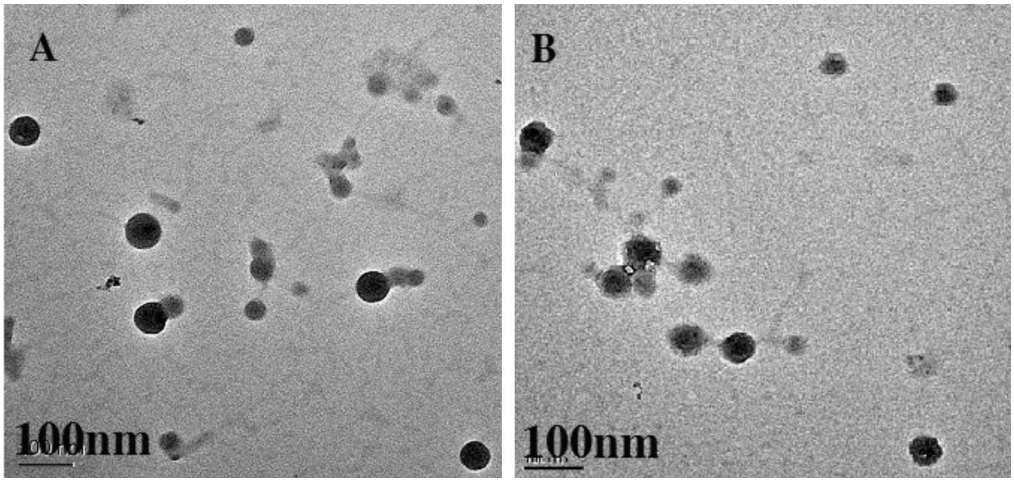

Fig. 4. TEM morphology of nanoparticles of *O,N*-CMCS-(Gly-Gly)$_3$-Me (5 mg/ml) in PBS (pH 7.4) solution. (A) Freshly prepared; (B) stored for one month.

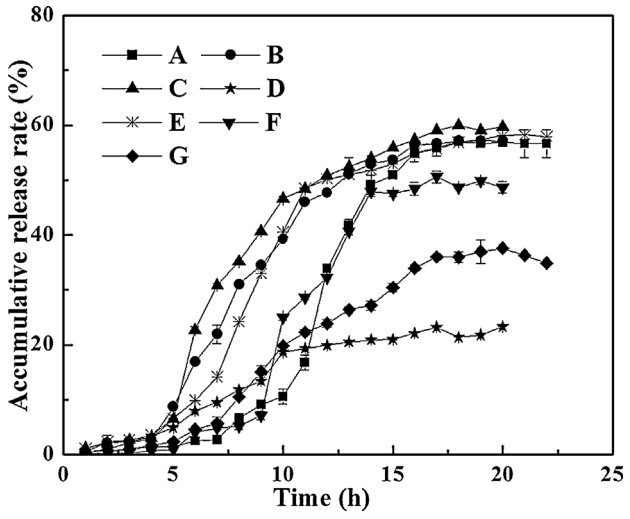

Fig. 5. Enzymatic degradation of polymer bound melphalan ((A) $M_w = 6.0 \times 10^4$ NPs with triple spacer incubated with tritosomes; (B) $M_w = 2.5 \times 10^7$ nanoparticles with triple spacer incubated with tritosomes; (C) $M_w = 3.4 \times 10^8$ nanoparticles with triple spacer incubated with tritosomes; (D) $M_w = 6.0 \times 10^4$ nanoparticles with triple spacer incubated with papain; (E) $M_w = 6.0 \times 10^4$ nanoparticles with quintuple spacer incubated with cathepsin X; (F) $M_w = 6.0 \times 10^4$ nanoparticles with triple spacer incubated with cathepsin X; (G) $M_w = 6.0 \times 10^4$ nanoparticles with single spacer incubated with cathepsin X).

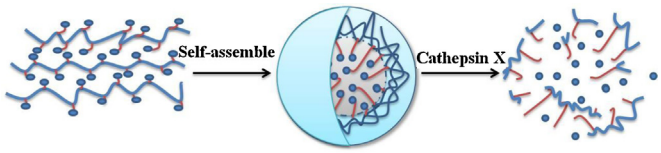

Fig. 6. Schematic illustration of the formation of self-assembled nanoparticles and the process of melphalan release.

degradation after swelling process, so the total amount of release drug was similar across all groups after 20 h.

Sustainable release of melphalan for a 24-h period suggests that *O,N*-CMCS-(Gly-Gly)$_3$-Me can be developed as potential anticancer agents.

3.4. Cytotoxicity of *O,N*-CMCS-(Gly-Gly)$_3$-Me

Fig. 7 is in vitro cell viability of multiple myeloma cells RPMI8226 incubated with different concentrations of melphalan or nanoparticles for 48 h. The cells incubated in culture media containing 30 μl tritosomes were also measured.

As showed in Fig. 7, free melphalan exhibits the maximum inhibition efficiencies while others have the lower values at each

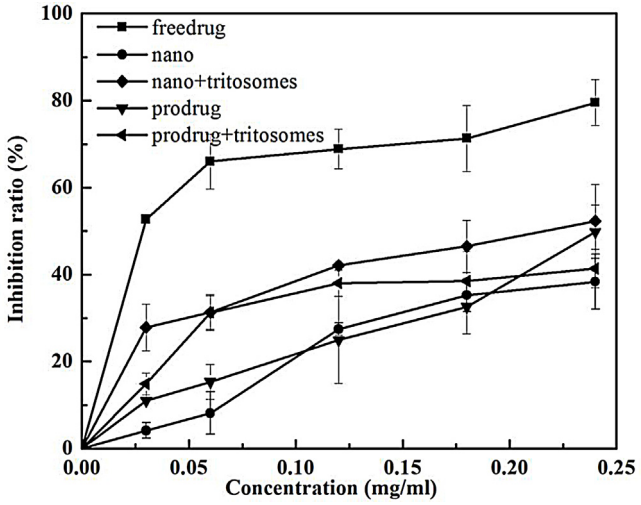

Fig. 7. Inhibition of RPMI-8226 cells proliferation by the compounds and melphalan after 48 h. All the experiments were performed in six times and average values were reported.

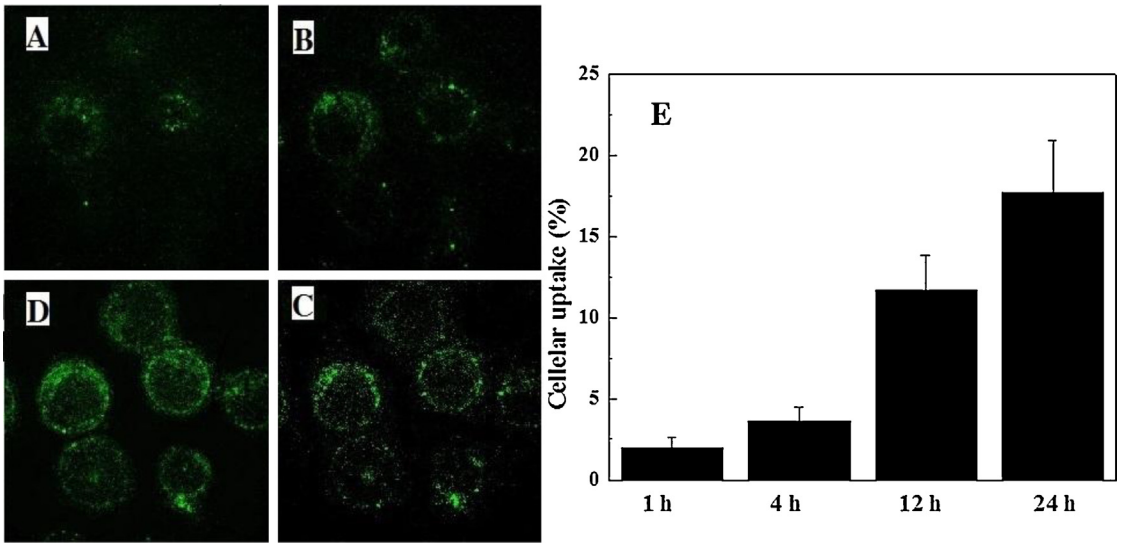

Fig. 8. Fluorescence images and intensity of *O*,*N*-CMCS-(Gly-Gly)$_3$-Me nanoparticles.((A) Fluorescent microscopy in 1 h; (B) fluorescent microscopy in 4 h; (C) fluorescent microscopy in 12 h; (D) fluorescent microscopy in 24 h; (E) fluorescence intensity).

concentration. The cytotoxicity was caused by drug-protein interactions. *O*,*N*-CMCS-(Gly-Gly)$_3$-Me are a kind of block copolymers composed of hydrophilic carboxymethyl and hydrophobic melphalan. Melphalan is chemically embedded in the interior core of the self-assembled nanoparticles, thus avoiding burst release. However, the nanostructures were destroyed by enzyme-mediated process, and more melphalan was released with larger inhibition ratios. These results indicate that the enzyme-sensitive polymer would be a useful tool for targeted cancer therapeutics.

3.5. *In vitro phagocytosis test*

The degree of cellular uptake was quantitatively characterized by fluorometric method by using Dylight-488 as a fluorescent probe, shown in Fig. 8. RPMI8226 cells were incubated with the nanoparticles for 1, 4, 12 and 24 h at 37 °C. From Fig. 8, it can be seen that the nanoparticles are effectively taken up by the cells. Nanoparticles were the most effective in the cellular uptake in comparison to all other formulations.

4. Conclusions

In this study, the targeted polymeric prodrug *O*,*N*-CMCS-(Gly-Gly)$_3$-Me was synthesized and self-assembled into nanoparticles in aqueous media. These polymers were evaluated as new drug delivery system and show suitable physicochemical properties for drug delivery. The selection of enzyme-sensitive spacers has important influence on the drug content and drug release behavior of polymeric prodrugs. In vitro study is shown that the conjugates degrade rapidly in cathepsin X media, which exhibited that the polymeric prodrug is a good cathepsin X-sensitive delivery system. These results illustrate that *O*,*N*-CMCS-(Gly-Gly)$_3$-Me is a prospective targeting drug delivery system for the treatment of multiple myeloma.

Acknowledgments

This project was supported by grants from the National Natural Science Foundation of China (51273156, 21204071), the Fundamental Research Funds for the Central Universities (WUT: 2013-IV-025), and the Natural Science Foundation of Hubei Province (2010CDA040) are gratefully acknowledged.

References

Anitha, A., Maya, S., Deepa, N., Chennazhi, K. P., Nair, S. V., Tamura, H., & Jayakumar, R. (2011). Efficient water soluble *O*-carboxymethyl chitosan nanocarrier for the delivery of curcumin to cancer cells. *Carbohydrate Polymers*, *83*(2), 452–461.

Bildstein, L., Dubernet, C., & Couvreur, P. (2011). Prodrug-based intracellular delivery of anticancer agents. *Advanced Drug Delivery Reviews*, *63*(1–2), 3–23.

Burke, P. J., Toki, B. E., Meyer, D. W., Miyamoto, J. B., Kissler, K. M., Anderson, M., Senter, P. D., & Jeffrey, S. C. (2009). Novel immunoconjugates comprised of streptonigrin and 17-amino-geldanamycin attached via a dipeptide-*p*-aminobenzyl-amine linker system. *Bioorganic Medicinal Chemistry Letters*, *19*(10), 2650–2653.

Cammas, S., Suzuki, K., Sone, C., Sakurai, Y., Kataoka, K., & Okano, T. (1997). Thermo-responsive polymer nanoparticles with a core-shell micelle structure as site-specific drug carriers. *Journal of Controlled Release*, *48*(2–3), 157–164.

Chhikara, B. S., Mandal, D., & Parang, K. (2010). Synthesis and evaluation of fatty acyl ester derivatives of cytarabine as anti-leukemia agents. *European Journal of Medicinal Chemistry*, *45*(10), 4601–4608.

Chrzanowski, K., Bielawska, A., & Pałka, J. (2003). Proline analogue of melphalan as a prodrug susceptible to the action of prolidase in breast cancer MDA-MB 231 cells. *Il Farmaco*, *58*(11), 1113–1119.

Devanathan, G., Turnbull, J. L., Ziomek, E., Purisima, E. O., Ménard, R., & Sulea, T. (2005). Carboxy-monopeptidase substrate specificity of human cathepsin X. *Biochemical and Biophysical Research Communications*, *329*(2), 445–452.

Dinauer, N., Balthasar, S., Weber, C., Kreuter, J., Langer, K., & Von Briesen, H. (2005). Selective targeting of antibody-conjugated nanoparticles to leukemic cells and primary T-lymphocytes. *Biomaterials*, *26*(29), 5898–5906.

Hjertner, Ö., Börset, M., & Waage, A. (1996). Comparison of the effects of 2-chlorodeoxyadenosine and melphalan on myeloma cell lines. *Leukemia Research*, *20*(2), 155–160.

Jain, K., Kesharwani, P., Gupta, U., & Jain, N. K. (2012). A review of glycosylated carriers for drug delivery. *Biomaterials*, *33*(16), 4166–4186.

Jeffrey, S. C., Nguyen, M. T., Andreyka, J. B., Meyer, D. L., Doronina, S. O., & Senter, P. D. (2006). Dipeptide-based highly potent doxorubicin antibody conjugates. *Bioorganic & Medicinal Chemistry Letters*, *16*(2), 358–362.

Jie, P., Venkatraman, S. S., Min, F., Freddy, B. Y. C., & Huat, G. L. (2005). Micelle-like nanoparticles of star-branched PEO–PLA copolymers as chemotherapeutic carrier. *Journal of Controlled Release*, *110*(1), 20–33.

Juan, S., & Bonifacino, M. D. (2009). *Current protocols in cell biology*. Bethesda, Maryland: John Wiley Sons, Inc.

Kirschke, H. (2007). *Cathepsin X*. Bergholz-Rehbrücke, Germany: Elsevier.

Liang, L., Lin, S., Dai, W., Lu, J., Yang, T., Xiang, Y., Zhang, Y., Li, R., & Zhang, Q. (2012). Novel cathepsin B-sensitive paclitaxel conjugate: Higher water solubility, better efficacy and lower toxicity. *Journal of Controlled Release*, *160*(3), 618–629.

Machana, S., Weerapreeyakul, N., Barusrux, S., Thumanu, K., & Tanthanuch, W. (2012). FTIR microspectroscopy discriminates anticancer action on human leukemic cells by extracts of *Pinus kesiya*; *Cratoxylum formosum* ssp. *pruniflorum* and melphalan. *Talanta*, *93*, 371–382.

Mahindra, A., Hideshima, T., & Anderson, K. C. (2010). Multiple myeloma: Biology of the disease. *Blood Reviews*, *24*(Suppl 1), S5–S11.

Mao, Z., Ma, L., Zhou, J., Gao, C., & Shen, J. (2005). Bioactive thin film of acidic fibroblast growth factor fabricated by layer-by-layer assembly. *Bioconjugate Chemistry*, *16*(5), 1316–1322.

Mincher, D. J., Van Valckenborgh, E., Young, L., Turnbull, A., Di Salvo, A., & Vanderkerken, K. (2008). Design of mechanisms of selective prodrug activation

in the bone marrow microenvironment of experimental and human multiple myeloma. *European Journal of Cancer Supplements*, *6*(9), 26.

Nägler, D. K., & Ménard, R. (1998). Human cathepsin X: A novel cysteine protease of the papain family with a very short proregion and unique insertions. *FEBS Letters*, *434*(1–2), 135–139.

Nägler, D. K., Zhang, R., Tam, W., Sulea, T., Purisima, E. O., & Ménard, R. (1999). Human Cathepsin X: A cysteine protease with unique carboxypeptidase activity. *Biochemistry*, *38*(39), 12648–12654.

Obermajer, N., Doljak, B., Jamnik, P., Fonović, U. P., & Kos, J. (2009). Cathepsin X cleaves the C-terminal dipeptide of alpha- and gamma-enolase and impairs survival and neuritogenesis of neuronal cells. *International Journal of Biochemistry & Cell Biology*, *41*(8–9), 1685–1696.

Ofner, C. M., III, Pica, K., Bowman, B. J., & Chen, C. (2006). Growth inhibition, drug load, and degradation studies of gelatin/methotrexate conjugates. *International Journal of Pharmaceutics*, *308*(1–2), 90–99.

Parekh, S., Weniger, M. A., & Wiestner, A. (2011). New molecular targets in mantle cell lymphoma. *Seminars in Cancer Biology*, *21*(5), 335–346.

Paulick, M. G., & Bogyo, M. (2011). Development of activity-based probes for cathepsin X. *ACS Chemical Biology*, *6*(6), 563–572.

Pinguet, F., Joulia, J. M., Martel, P., Grosse, P. Y., Astre, C., & Bressolle, F. (1996). High-performance liquid chromatographic assay for melphalan in human plasma application to pharmacokinetic studies. *Journal of Chromatography B: Biomedical Sciences and Applications*, *686*(1), 43–49.

Rajpoot, P., Bali, V., & Pathak, K. (2012). Anticancer efficacy, tissue distribution and blood pharmacokinetics of surface modified nanocarrier containing melphalan. *International Journal of Pharmaceutics*, *426*(1–2), 219–230.

Ruth, D., Isabella, C. H., Harold, J. Y., Pauline, A. F., Karel, U., Vladimir, S., & Jiri, S. (1991). Macromolecular prodrugs for use in targeted cancer chemotherapy: Melphalan covalently coupled to *N*-(2-hydroxypropyl) methacrylamide copolymers. *Journal of Controlled Release*, *16*, 121–136.

She, W., Luo, K., Zhang, C., Wang, G., Geng, Y., Li, L., He, B., & Gu, Z. (2013). The potential of self-assembled, pH-responsive nanoparticles of mPEGylated peptide dendron–doxorubicin conjugates for cancer therapy. *Biomaterials*, *34*(5), 1613–1623.

Sun, L., Zhao, Y., Li, X., Yuan, H., Cheng, A., & Lou, H. (2010). A lysosomal–mitochondrial death pathway is induced by solamargine in human K562 leukemia cells. *Toxicology in Vitro*, *24*(6), 1504–1511.

Vig, B. S., Huttunen, K. M., Laine, K., & Rautio, J. (in press). Amino acids as promoieties in prodrug design and development. *Advanced Drug Delivery Reviews*. 65 (10), 2013, 1370–1385.

Wickström, M., Viktorsson, K., Lundholm, L., Aesoy, R., Nygren, H., Sooman, L., Fryknäs, M., Vogel, L. K., Lewensohn, R., Larsson, R., & Gullbo, J. (2010). The alkylating prodrug J1 can be activated by aminopeptidase N, leading to a possible target directed release of melphalan. *Biochemical Pharmacology*, *79*(9), 1281–1290.

Wu, Z., Shah, A., Patel, N., & Yuan, X. (2010). Development of methotrexate proline prodrug to overcome resistance by MDA-MB-231 cells. *Bioorganic & Medicinal Chemistry Letters*, *20*(17), 5108–5112.

Zheng, H., Rao, Y., Yin, Y., Xiong, X., Xu, P., & Lu, B. (2011). Preparation, characterization, and in vitro drug release behavior of 6-mercaptopurine-carboxymethyl chitosan. *Carbohydrate Polymers*, *83*(4), 1952–1958.